Vol. 85 (1994) *ACTA PHYSICA POLONICA A* No. 5

SUPERIONIC PHASE TRANSITION IN $Rb_4LiH_3(SeO_4)_4$ SINGLE CRYSTALS *

M. Połomska, B. Hilczer, J. Wolak

Institute of Molecular Physics, Polish Academy of Sciences
Smoluchowskiego 17/19, 60-179 Poznań, Poland

and A. Pietraszko

Institute of Low Temperature Physics and Structural Research
Polish Academy of Sciences
Okólna 1, 50-950 Wrocław, Poland

(Received November 30, 1993; in final form March 1, 1994)

Derivatographic, dielectric and complex impedance studies of $Rb_4LiH_3(SeO_4)_4$ crystals revealed a superionic phase transition at $T_s \approx 448$ K. The bulk conductivity rises from 10^{-6} to 10^{-4} $(\Omega m)^{-1}$ at T_s, and the activation energy of conductivity in the direction of crystal axes a and b (where $a = b$ for tetragonal symmetry) $W_a = W_b$ decreases from 0.94 eV in the low temperature phase to the value of 0.27 eV at $T > T_s$. The analysis of the results of X-ray studies at room temperature and at 450 K indicates that the fast ion transport, characterized by low activation energy, is related to the delocalization of the H2 protons in the O(12)–H2–O(24) bonds linking the $Se(1)O_4$ and $Se(2)O_4$ tetrahedra. The "cogwheel" mechanism is suggested to be involved in the fast proton transport.

PACS numbers: 61.50.Em, 62.20.Dc, 77.22.Gm

1. Introduction

$Rb_4LiH_3(SeO_4)_4$, denoted as RLHSe, belongs to a new family of compounds of the general formula $Me_4LiH_3(XO_4)_4$, where Me = Rb, K, NH_4 and X = S or Se. Although the existence of crystals of the above-mentioned stoichiometry was reported more than a hundred years ago [1], it was only recently that the crystals aroused the interest of scientists owing to their ferroelastic properties. The $Rb_4LiH_3(SO_3)_4$ crystals were found to be ferroelastic below 137 K [2, 3], whereas the ferroelastic–paraelastic phase transition was observed in RLHSe crystals at 100 K [4, 5]. The crystals of both compounds are isomorphous and have tetragonal

*The work was supported by the grant no. 2 0977 91 01 from the Committee for Scientific Research.

symmetry at room temperature (space group $P4_1$) [6–8], with four formula units in an elementary unit cell and the following unit cell parameters: $a = 7.836$ Å, $c = 30.273$ Å for $Rb_4LiH_3(SO_4)_4$ and $a = 7.623$ Å, $c = 29.483$ Å for RLHSe.

In the present paper we report the results of our thermal, dielectric and electric studies of RLHSe single crystals in the temperature range above room temperature. The results are discussed on the basis of the crystal structure solved both at room temperature and at 450 K.

2. Experimental

RLHSe single crystals were grown at room temperature from aqueous solution of Li_2CO_3 and Rb_2CO_3, in the molar ratio 1:4, and an amount of H_2SeO_4 to settle the pH value of the solution below 1. The habitus of RLHSe single crystals is shown in Fig. 1.

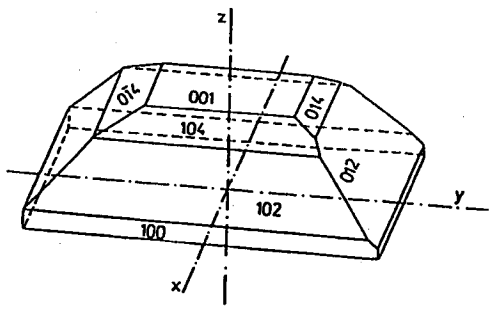

Fig. 1. Habitus of $Rb_4LiH_3(SeO_4)_4$ single crystals.

The samples, ≈ 0.5 mm thick and a few mm^2 in area, were cut perpendicularly to the crystallographic axes, gold electrodes were evaporated onto the sample surfaces. Temperature variation in the capacitance was measured in the frequency range 1 kHz–1 MHz using HP-4270A automatic bridge. The impedance spectroscopy was used to study temperature variation in the electric conductivity. The complex impedance Z^* was measured by means of Tesla BM 507 Impedance Meter in the frequency range 5 Hz–500 kHz. During the measurements the temperature was stabilized with an accuracy of 0.01 K by using a specially constructed heating stage controlled by Unipan 655 temperature controller.

Differential thermal analysis (DTA), thermogravimetric (TG) and differential thermogravimetric (DTG) studies of RLHSe crystals were performed above room temperature by using the Paulik–Paulik system at various heating rates.

The crystal structure of RLHSe was determined at room temperature and at 450 K by using four-cycle X-ray diffractometer (KM-4). The temperature of the sample was stabilized with an accuracy of 0.2. SHELXL-93 program was used to refine the crystal structure.

3. Results

3.1. Thermal studies

Figure 2 shows the results of DTA, TG and DTG studies of RLHSe crystal. DTG curve indicates that the crystal starts to decompose at about 495 K. Two endothermic peaks at $T_2 = 437$ K and $T_1 = 486$ K are visible below the decomposition temperature. Detailed studies revealed that the DTA peak at T_2 is reversible when the crystal is not heated above 490 K, and can be ascribed to a phase transition. Moreover, we found that the entropy change at T_2 was rather inconspicuous, amounting to $\Delta S \approx 0.5$ J/mol K.

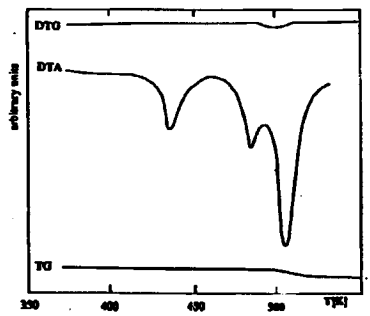

Fig. 2. Results of differential thermal analysis (DTA), thermogravimetric (TG) and differential thermogravimetric (DTG) studies of $Rb_4LiH_3(SeO_4)_4$ single crystals; heating rate $dT/dt = 10$ K/min.

3.2. Dielectric studies

Dielectric measurements revealed an anomalous increase in the capacitance of RLHSe samples at about 445 K, when measured at the frequencies 1–100 kHz. Figure 3 shows temperature variation in dielectric permittivity along the a-axis measured at the frequency 1 kHz. An anomalous increase, with a maximum at about 451 K, is observed in permittivity on heating. At about 460 K another permittivity maximum is visible. The permittivity decreases on cooling the sample, and in the low temperature anomaly region a thermal hysteresis of a few degrees is observed. This implies that the phase transition at about 450 K is of the first order.

As the dielectric anomaly observed in RLHSe crystals was similar to that observed by us at the superionic phase transition in $CsHSeO_4$ crystals [9], we performed complex impedance measurements of RLHSe crystals at various temperatures. Figures 4 and 5 show the $Z''(Z')$ plots at various temperatures measured along the b- and c-axes. The $Z''(Z')$ plots measured along the a-axis were very close to those obtained for the b-direction. The experimental points in the $Z''(Z')$ plots obtained in the three crystallographic directions form semicircles beginning

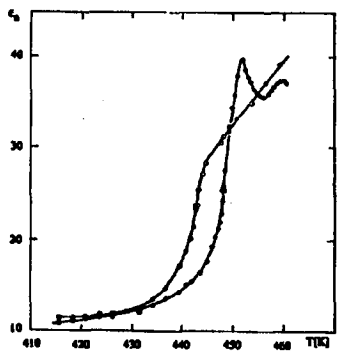

Fig. 3. Temperature variation of dielectric permittivity measured along the a-axis ($f = 1$ kHz) on heating and on cooling.

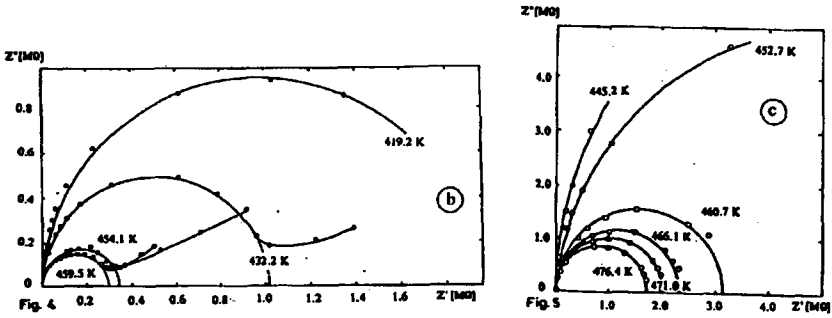

Fig. 4. Complex plane impedance diagrams at various temperatures of $Rb_4LiH_3(SeO_4)_4$ crystal along the b-axis.
Fig. 5. Complex plane impedance diagrams at various temperatures for $Rb_4LiH_3(SeO_4)_4$ crystal along the c-axis.

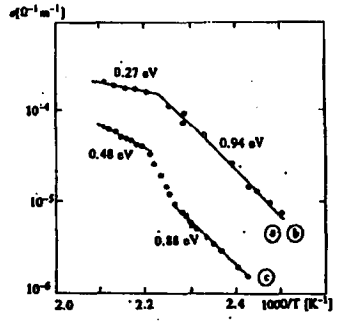

Fig. 6. Temperature variation of the bulk conductivity of $Rb_4LiH_3(SeO_4)_4$ crystal along tetragonal axes.

at the origin of the coordinates. The diameter of each semicircle at corresponding temperature was taken as the measure of the bulk resistance of the sample. Figure 6 shows a temperature variation of conductivity along three crystallographic directions. It is evident that the conductivity along the a- and b-axes is the same and higher than that along the c-axis. The activation energies $W_a = W_b = 0.94$ eV and $W_c = 0.88$ eV are obtained below the temperature of about 448 K. Above this temperature a decrease in the activation energy to the values of $W_a = W_b = 0.27$ eV and $W_c = 0.48$ eV can be observed. Moreover, in the phase transition region a deviation from Arrhenius law is observed along the c-axis.

3.3. Crystal structure

$Rb_4LiH_3(SeO_4)_4$ crystals have a tetragonal symmetry (space group $P4_1$) with four chemical units forming the room temperature unit cell. The structure consists of sandwiches of SeO_4 tetrahedra, with Rb^+ ions in between, stacked along the c-tetragonal axis (Figs. 7, 8). Two layers consisting of SeO_4 groups form a sandwich. The SeO_4 tetrahedra contained in the two layers are connected by hydrogen bonds O(32)–H1–O(41) and O(12)–H2–O(24), respectively, whereas the hydrogen bond O(22)–H3–O(34) links the layers in a sandwich. The SeO_4 tetrahedra in consecutive, identical sandwiches are turned by 90° around the fourfold axis. Li^+ ions are located between the sandwiches.

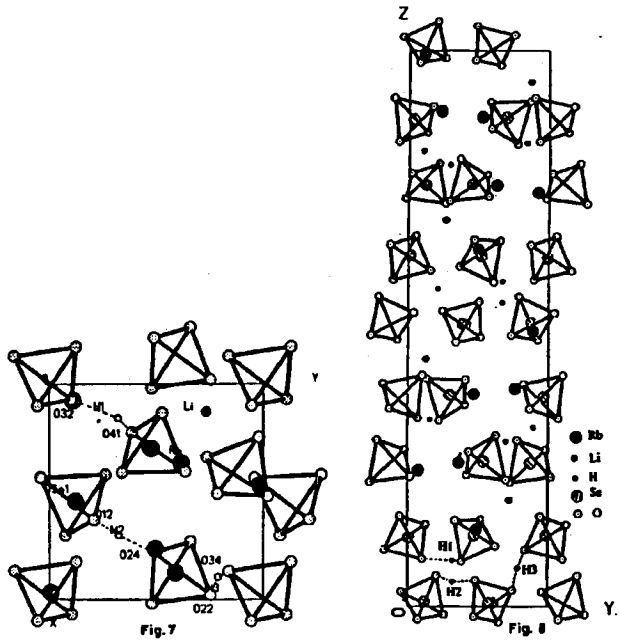

Fig. 7. (ab) projection of the $Rb_4LiH_3(SeO_4)_4$ crystal structure.
Fig. 8. (bc) projection of the $Rb_4LiH_3(SeO_4)_4$ crystal structure.

TABLE I

Se–O distances in four SeO_4 tetrahedra of $Rb_4LiH_3(SeO_4)_4$ crystals at room temperature and at 450 K.

	Distances [Å] at room temperature	Distances [Å] at 450 K
Se1 – O(11)	1.615	1.589
– O(12)	1.706	1.676
– O(13)	1.609	1.598
– O(14)	1.622	1.603
Se2 – O(21)	1.609	1.596
– O(22)	1.675	1.667
– O(23)	1.587	1.564
– O(24)	1.612	1.615
Se3 – O(31)	1.603	1.642
– O(32)	1.628	1.622
– O(33)	1.630	1.615
– O(34)	1.668	1.664
Se4 – O(41)	1.698	1.714
– O(42)	1.607	1.617
– O(43)	1.614	1.606
– O(44)	1.602	1.589

TABLE II

Proton–oxygen distances of hydrogen bonds in $Rb_4LiH_3(SeO_4)_4$ at room temperature and at 450 K.

	Distances [Å] at room temperature	Distances [Å] at 450 K
H1 – O(32)	1.903	1.516
– O(41)	0.701	0.980
H2 – O(12)	1.133	1.334
– O(24)	1.449	1.221
H3 – O(22)	1.420	0.799
– O(34)	1.136	1.827

Above the phase transition temperature the crystal is still tetragonal and characterized by the same $P4_1$ space group. However, the SeO_4 tetrahedra undergo a change. The changes in the Se–O bond length of all tetrahedra (Table I) induce

changes in the hydrogen bonds linking the SeO_4 tetrahedra in a layer and the two layers in a sandwich. Table II shows O–H–O distances in the three hydrogen bonds obtained from X-ray measurements at room temperature and at 450 K. It should be noted, however, that in the temperature range studied the Li-ions change their position only slightly.

4. Discussion

Many crystals of various hydrogen sulphates and selenates were found to exhibit protonic conduction and superionic phase transition [10–23], however, the conductivity changes at the phase transition temperature T_s and the activation energies in the superionic phase are very different. The conductivity jump at T_s in a simple selenate $CsHSeO_4$ was of about four orders of magnitude, and a small activation energy $W_a = W_b = W_c = 0.10$ eV was obtained in the superionic phase [18]. The $Me_3H(SeO_4)_2$ family exhibits a conductivity jump of about one order of magnitude at T_s, with activation energies $W_a = W_b = 0.26$–0.39 eV in the high conducting phase, depending on the crystal [16, 17, 20–22]. Conductivity jump at T_s, of more than three orders of magnitude, and low activation energy in the superionic phase $W_a = W_b = W_c = 0.11$ eV were also found in $(NH_4)_4H_2(SeO_4)_3$ [15].

We observed that the $Rb_4LiH_3(SeO_4)_4$ crystals undergo the first order phase transition at about 448 K. At this temperature the activation energies of electric conductivity decrease considerably to the value of $W_a = W_b = 0.27$ eV, comparable to that found in the superionic phase of other hydrogen selenates exhibiting similar anisotropy of conductivity, i.e. $Me_3H(SeO_4)_2$ crystals. Thus, taking into account the low activation energy of the conductivity above 448 K, and the anomalous dielectric behaviour at this temperature (Fig. 3), we classify the transition to be a superionic one. However, it should be noted that there are some differences between the properties of RLHSe crystals and the above-mentioned selenates. The conductivity values just above the superionic transition of the latter are considerably higher than those of RLHSe crystals (Fig. 9). Moreover, the above-mentioned

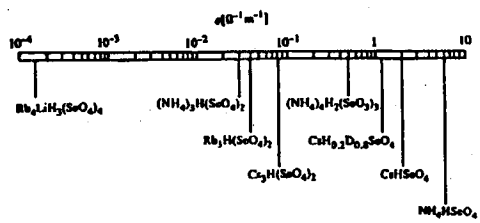

Fig. 9. Electric conductivities of various hydrogen selenates just above superionic phase transition $T \geq T_s$ (our results).

crystals undergo a superionic phase transition at the temperature, where they lose the ferroelastic properties, whereas the ferroelastic–paraelastic phase transition temperature in RLHSe lies far below T_s [4, 5].

X-ray studies revealed that the RLHSe crystals show no changes in the space group, during the phase transition, however, the Se–O distances of the four different SeO_4 tetrahedra are little bit diversified (Table I). This induces changes in the hydrogen bonds (Table II). The O(32)···H1–O(41) bond becomes more symmetrical at $T > T_s$, but the H1 proton is still strongly bonded to the O(41) oxygen. Above T_s the proton H3 changes its position in the O(22)···H3–O(34) bond, so that its bonding to the O(22) oxygen results in the asymmetry of the electric charge in the neighbourhood. The O(12)–H2···O(14) bond becomes symmetrical above T_s. Thus the proton H2 can be treated as delocalized and involved in the fast proton transport. Thermal studies of $Cs_3H(SeO_4)_2$ crystals [23] pointed to the model where the short range order of protons surrounding plays the main role at the superionic phase transition. The entropy change $\Delta S = 0.5$ J/mol observed in RLHSe crystals at T_s is small compared with the values of 9.4 J/mol and 43. J/mol found in $Cs_3H(SeO_4)_2$ and $(NH_4)_4H_2(SeO_4)_3$ crystals, respectively [23, 24]. The low value of entropy change of RLHSe crystals is in agreement with small changes of local structure observed at T_s.

The results of our studies show that RLHSe crystals undergo the first order superionic phase transition at $T_s = 448$ K. The fast proton transport in the superionic phase is related to the delocalization of H2 proton in the O(12)–H2–O(24) bond. The "cogwheel" mechanism [25] resulting from a coupled rotation of sulphate ions can be assumed to be responsible for the fast proton transport in the (a, b) plane of RLHSe crystals. One of the arguments for this mechanism is the fact that only the changes in the close surrounding of protons are responsible for the superionic phase transition. The evidence for this are the results of X-ray studies and entropy changes at T_s. The small conductivity value in the RLHSe crystals can be explained by the fact that only the H2 proton can be involved in the fast proton transport.

References

[1] A. Scacchi, *Mem. Acc. d Sc. Fis. Mat. Napoli* **3**, Sep. 48 (1867), after P. Groth, *Chemische Kristallographie*, Vol. 2, Engelman Verlag, Leipzig 1908, p. 311.

[2] T. Wołejko, P. Piskunowicz, T. Bręczewski, T. Krajewski, *Ferroelectrics* **81**, 175 (1988).

[3] B. Mróz, H. Kiefte, M.J. Clouter, *Ferroelectrics* **82**, 105 (1988).

[4] M. Połomska, F. Smutny, *Phys. Status Solidi B* **154**, K103 (1989).

[5] M. Połomska, F. Smutny, *Ferroelectrics* **111**, 237 (1990).

[6] A. Pietraszko, K. Łukaszewicz, *Z. Kristallogr.* **185**, 564 (1988).

[7] F.J. Zuniga, G. Extebaria, G. Madariaga, T. Bręczewski, *Acta Crystallogr. C* **46**, 1199 (1990).

[8] A. Pietraszko, M. Połomska, A. Pawłowski, *Izv. Akad. Nauk SSSR, Ser. Fiz.* **55**, 520 (1991).

[9] J. Wolak, Z. Czapla, *Phys. Status Solidi A* **67**, K171 (1981).

[10] A.I. Baranov, L.A. Shuvalov, N.M. Schagina, *Pis'ma Zh. Eksp. Teor. Fiz.* **36**, 381 (1982).

[11] A.I. Baranov, R.M. Fedosyuk, N.M. Schagina, L.A. Shuvalov, *Ferroelectr. Lett.* **2**, 25 (1984).

[12] R. Blinc, J. Dolinsek, G. Lahajnar, I. Zupanic, L.A. Shuvalov, A.I. Baranov, *Phys. Status Solidi B* **123**, K83 (1984).

[13] Yu.N. Moskvich, O.V. Rozanov, A.A. Sukhovsky, I.P. Aleksandrova, *Ferroelectrics* **63**, 83 (1985).

[14] M. Pham-Thi, Ph. Colomban, A. Novak, R. Blinc, *Solid State Commun.* **55**, 265 (1985).

[15] Cz. Pawlaczyk, F.E. Salman, A. Pawłowski, Z. Czapla, A. Pietraszko, *Phase Transit.* **8**, 9 (1986).

[16] A.I. Baranov, I.P. Makarova, L.A. Muradyan, A.V. Tregubchenko, L.A. Shuvalov, V.I. Simonov, *Kristallografiya* **32**, 682 (1987).

[17] A.I. Baranov, A.V. Tregubchenko, L.A. Shuvalov, N.M. Schagina, *Fiz. Tverd. Tela* **29**, 2313 (1987).

[18] B. Hilczer, Cz. Pawlaczyk, F.E. Salman, *Ferroelectrics* **81**, 195 (1988).

[19] A. Pawłowski, Cz. Pawlaczyk, *Ferroelectrics* **81**, 201 (1988).

[20] B.V. Merinov, A.I. Baranov, L.A. Shuvalov, *Kristallografiya* **35**, 355 (1990).

[21] D. Abramič, J. Dolinšek, R. Blinc, L.A. Shuvalov, *Phys. Rev. B* **42**, 442 (1990).

[22] A. Pawłowski, Cz. Pawlaczyk, B. Hilczer, *Solid State Ionics* **44**, 17 (1990).

[23] B. Hilczer, A. Pawłowski, *Ferroelectrics* **104**, 383 (1990).

[24] L. Szcześniak, B. Hilczer, A. Pawłowski, to be published.

[25] R. Aronson, B. Jansson, H.E.G. Knape, A. Lunden, L. Nilsson, C.A. Sjöblon, L.M. Torell, *J. Phys. (France)* **41**, C6-35 (1980).